REPORT DOCUMENTATION PAGE

Form Approved OMB NO. 0704-0188

1. REPORT DATE (DD-MM-YYYY) 08-09-2019	2. REPORT TYPE Final Report	3. DATES COVERED (From - To) 15-Mar-2016 - 14-Jun-2019

4. TITLE AND SUBTITLE
Final Report: Multiscale and Correlated Dynamic Adaptive Chemistry and Transport Modeling of Ignition and Flame Regimes of Stratified Fuel Mixtures

5a. CONTRACT NUMBER
W911NF-16-1-0076

5b. GRANT NUMBER

5c. PROGRAM ELEMENT NUMBER
611102

6. AUTHORS

5d. PROJECT NUMBER

5e. TASK NUMBER

5f. WORK UNIT NUMBER

7. PERFORMING ORGANIZATION NAMES AND ADDRESSES
Princeton University
PO Box 36
87 Prospect Avenue, Second Floor
Princeton, NJ 08544 -2020

8. PERFORMING ORGANIZATION REPORT NUMBER

9. SPONSORING/MONITORING AGENCY NAME(S) AND ADDRESS (ES)
U.S. Army Research Office
P.O. Box 12211
Research Triangle Park, NC 27709-2211

10. SPONSOR/MONITOR'S ACRONYM(S)
ARO

11. SPONSOR/MONITOR'S REPORT NUMBER(S)
66699-EG.11

12. DISTRIBUTION AVAILIBILITY STATEMENT
Approved for public release; distribution is unlimited.

13. SUPPLEMENTARY NOTES
The views, opinions and/or findings contained in this report are those of the author(s) and should not contrued as an official Department of the Army position, policy or decision, unless so designated by other documentation.

14. ABSTRACT

15. SUBJECT TERMS

16. SECURITY CLASSIFICATION OF:			17. LIMITATION OF ABSTRACT	15. NUMBER OF PAGES	19a. NAME OF RESPONSIBLE PERSON
a. REPORT	b. ABSTRACT	c. THIS PAGE			Yiguang Ju
UU	UU	UU	UU		19b. TELEPHONE NUMBER 609-258-5644

Standard Form 298 (Rev 8/98)
Prescribed by ANSI Std. Z39.18

RPPR Final Report
as of 16-Sep-2019

Agency Code:

Proposal Number: 66699EG **Agreement Number: W911NF-16-1-0076**

INVESTIGATOR(S):

Name: Yiguang Ju
Email: yju@princeton.edu
Phone Number: 6092585644
Principal: Y

Organization: **Princeton University**
Address: PO Box 36, Princeton, NJ 085442020
Country: USA
DUNS Number: 002484665 EIN: 210634501

Report Date: 14-Sep-2019 Date Received: 08-Sep-2019

Final Report for Period Beginning 15-Mar-2016 and Ending 14-Jun-2019

Title: Multiscale and Correlated Dynamic Adaptive Chemistry and Transport Modeling of Ignition and Flame Regimes of Stratified Fuel Mixtures

Begin Performance Period: 15-Mar-2016 **End Performance Period:** 14-Jun-2019

Report Term: 0-Other

Submitted By: Yiguang Ju Email: yju@princeton.edu
Phone: (609) 258-5644

Distribution Statement: 1-Approved for public release; distribution is unlimited.

STEM Degrees: 2 **STEM Participants:** 0

Major Goals: Advanced engines need to operate at higher boosted pressure, lower temperature, and variety of alternative fuels for higher energy efficiency, higher power, more fuel flexibility, and less emissions. However, at higher pressures, low temperature chemistry plays a critical role in affecting engine performance, engine knocking, combustion processes, and results in strong turbulence/chemistry interaction as well as new ignition and flame regimes. Quantitative modeling of such complicated reactive flow at extreme conditions requires detailed models for chemical kinetics and transport, and thus is extremely challenging. The goal of this proposal is to develop a hybrid multi-timescale and correlated dynamic adaptive chemistry and transport (HMTS/CO-DACT) method for accurate and computationally-efficient modeling of low temperature ignition and knock formation of surrogate diesel fuel mixtures.

Accomplishments: In this project, we developed a hybrid multi-timescale and correlated dynamic adaptive chemistry and transport (HMTS/CO-DACT) method for accurate and computationally-efficient modeling of low temperature ignition and knock formation of surrogate diesel fuel mixtures. The results showed that the present CO-DACT method is very computationally efficient to handle detailed chemical kinetics and multi-species transport properties. The method was successfully applied not only to low temperature and high temperature ignition and flame modeling but also to the simulations of engine knocking. The results show clearly that not only low temperature chemistry but also its interaction with turbulence significantly affect knock formation. By considering both the temperature and fuel concentration gradients, an engine knock regime diagram with and without low temperature chemistry is obtained. The result outcome not only provides a computationally efficient tool for engine modeling and fuel design but also advances the understanding of role of low temperature chemistry in knock formation.

Training Opportunities: The project provides research opportunities for four graduate students and one postdoc fellow for their career development.

Results Dissemination: The results are published on technical journals and conferences as following:

Technical Papers

1. Weiqi Sun and Yiguang Ju, (2017); A multi-timescale and correlated dynamic adaptive chemistry and transport (CO-DACT) method for computationally efficient modeling of jet fuel combustion with detailed chemistry and transport, Combustion and Flame 184 (2017) 297–311.
2. Tianhan Zhang, Weiqi Sun, Yiguang Ju, (2017); Multi-scale Modeling of Detonation Formation with Concentration and Temperature Gradients in n-Heptane/Air Mixtures, Proceedings of the Combustion Institute, 36 (1), pp.1539-1547.
3. Mao, X., Rousso, A., Chen, Q. and Ju, Y., 2018. Numerical modeling of ignition enhancement of CH4/O2/He mixtures using a hybrid repetitive nanosecond and DC discharge. Proceedings of the Combustion Institute, Vol.37, 1-8. https://doi.org/10.1016/j.proci.2018.05.106
4. Zhang, T., Zhao, H. and Ju, Y., 2018. Numerical Studies of Novel Inwardly Off-Center Shearing Jet-Stirred Reactor. AIAA Journal, 56, pp.1-5. https://doi.org/10.2514/1.J057293
5. Liu, Z., Han, W., Kong, W. and Ju, Y., 2018. LES modelling of turbulent non-premixed jet flames with correlated dynamic adaptive chemistry. Combustion Theory and Modelling, 22, pp.1-20. https://doi.org/10.1080/13647830.2018.1447148
6. Yiguang Ju, Christopher B. Reuter, Omar R. Yehia, Tanvir I. Farouk, and Sang Hee Won, Dynamics of Cool Flames, Progress of Energy and Combustion Science, 75 (2019), 100787. https://doi.org/10.1016/j.pecs.2019.100787.
7. Omar Yehia et al., Kinetic effects of n-propylbenzene on n-dodecane counterflow nonpremixed cool flames, Combustion and Flame, 208:262-272, 2019, https://doi.org/10.1016/j.combustflame.2019.07.006.
8. Tianhan Zhang, Weiqi Sun, Liang Wang, Yiguang Ju, “Effects of Low-Temperature Chemistry and Turbulent Transport on Knocking Formation for Stratified Dimethyl Ether/Air Mixtures, Combustion and Flame, Vol.200, 2019: 342-353.
9. Alex G. Novoselov, , Christopher B. Reuter, Omar R. Yehia, Sang Hee Won, Matthew K. Fu, Katherine A. Kokmanian, Marcus Hultmark, Yiguang Ju, Michael E. Mueller, Turbulent nonpremixed cool flames: Experimental measurements, Direct Numerical Simulation, and manifold-based combustion modeling, Combustion and Flame, 209: 144-154, 2019, https://doi.org/10.1016/j.combustflame.2019.07.034

Conference papers

1. W. Sun, Y. Ju, Multi-timescale and Correlated Dynamic Adaptive Chemistry and Transport (CO-DACT) modeling of ignition and flame propagation of jet fuel surrogate mixtures, 9th U.S. National Combustion Meeting, 17 May 2015, Cincinnati, Ohio.
2. Yiguang Ju, Christopher B. Reuter, Numerical Simulations of Cool Flame Propagation Limits and Speeds at Elevated Pressures (AIAA 2016-0444), 54th AIAA Aerospace Sciences Meeting, 2016, 10.2514/6.2016-0444
3. Weiqi Sun, Yiguang Ju, A Smart CSP Method and Correlated Dynamic Adaptive Chemistry and Transport Algorithm for Computationally Efficient Modeling with A Detailed Mechanism (AIAA 2016-1208), 54th AIAA Aerospace Sciences Meeting, 2016, 10.2514/6.2016-1208.
4. W. Sun, Y. Ju, A smart CSP method and correlated dynamic adaptive chemistry and transport modeling with hydrogen/air mixtures, 2016 SPRING TECHNICAL MEETING, EASTERN STATES SECTIONS OF THE COMBUSTION INSTITUTE, Princeton University, New Jersey, March 13-16, 2016.
5. Y. Ju, Dynamics and burning limits of premixed cool flames at high pressures, 2016 SPRING TECHNICAL MEETING, EASTERN STATES SECTIONS OF THE COMBUSTION INSTITUTE, Princeton University, New Jersey, March 13-16, 2016.
6. Y. Ju, Propagation Limits of High Pressure Cool Flames, DFD16-2016-001961, 69th Annual Meeting of the APS Division of Fluid Dynamics, Oregon, Nov.20. 2016.
7. Weiqi Sun, Temistocle Grenga, Yiguang Ju, Hybrid Multi-Timescale and G-Scheme Method for Efficient Modeling with Detailed Chemical Kinetics (AIAA 2017-0602), 55th AIAA Aerospace Sciences Meeting, 2017, 10.2514/6.2017-0602
8. Yiguang Ju, Eric Lin, Christopher B. Reuter, The effect of radiation on the dynamics of near limit cool flames and hot flames (AIAA 2017-1965), 55th AIAA Aerospace Sciences Meeting, 2017, 10.2514/6.2017-1965
9. W. Sun, L. Wang, T. Grenga, Y. Ju, Comparative study of hybrid multi-timescale and G-Scheme methods for MARCS with detailed chemical kinetics, 10th U.S. National Combustion Meeting, College Park, Maryland, Sunday, 23 April 2017.
10. W. Sun, L. Wang, T. Grenga, Y. Ju, Development of a Multiscale Adaptive Reduced Chemistry Solver (MARCS) for Computationally Efficient Combustion Simulations (Paper 1081) 26th International Colloquium on the Dynamics of Explosions and Reactive Systems (ICDERS), Boston, USA, 30 July – 4 August 2017.

11. Eric Lin, Christopher B. Reuter and Yiguang Ju, The effect of radiation on the dynamics of near limit diffusion cool flames and hot flames, 71st Annual Meeting of the APS Division of Fluid Dynamics, Denver, November 18-20, 2018.
12. Novoselov A, Reuter C, Yehia O, Ju Y, Mueller M. Computational and Experimental Investigation of Turbulent Nonpremixed Cool Flames. Bulletin of the American Physical Society. 2018 Nov 20.
13. Zhang, T., Grenga, T. and Ju, Y., 2018. A comprehensive multi-scale method of model reduction and analysis for reactive flow. Bulletin of the American Physical Society.
14. Omar Yehia, Christopher B. Reuter, and Yiguang Ju. "On low-temperature ether multistage flames", 2018 AIAA Aerospace Sciences Meeting, AIAA SciTech Forum, (AIAA 2018-2185) https://doi.org/10.2514/6.2018-2185.
15. Tianhan Zhang, Yiguang Ju, and Hao Zhao. "Numerical Studies of the Residence Time Distributions of an Inwardly Off-center Shearing Jet Stirred Reactor (IOS-JSR)", 2018 AIAA Aerospace Sciences Meeting, AIAA SciTech Forum, (AIAA 2018-1670) https://doi.org/10.2514/6.2018-1670.
16. O.R. Yehia, C.B. Reuter, Y. Ju Low-temperature multistage diffusion flames, 2018 SPRING TECHNICAL MEETING, EASTERN STATES SECTIONS OF THE COMBUSTION INSTITUTE, The Pennsylvania State University, Pennsylvania, March 4-7, 2018.
17. T. Zhang, W. Sun, L. Wang, Y. Ju, Effects of thermal and fuel stratifications and turbulence transport on knocking formation for dimethyl ether/air mixtures, 2018 SPRING TECHNICAL MEETING, EASTERN STATES SECTIONS OF THE COMBUSTION INSTITUTE, The Pennsylvania State University, Pennsylvania, March 4-7, 2018
18. A.G. Novoselov, C.B. Reuter, O.R. Yehia, Y. Ju, M. E. Mueller, Do turbulent nonpremixed cool flames require special treatment? 11th U.S. National Combustion Meeting, Pasadena, California, March 24-26, 2019.
19. T. Zhang, W. Sun, L. Wang, Y. Ju, Effects of low-temperature chemistry and turbulent transport on knocking formation for stratified dimethyl ether/air mixtures, 11th U.S. National Combustion Meeting, Pasadena, California, March 24-26, 2019.
20. Hossam A. El-Asrag and Yiguang Ju, "Direct Numerical Simulation of Exhaust Gas Recirculation Effect on Autoignition of an HCCI Stratified Turbulent Flow Field for DME/Air mixture at High Pressure: NO effect," AIAA 2013-1047, 51st AIAA Aerospace Sciences Meeting including the New Horizons Forum and Aerospace Exposition, 07 - 10 January 2013, Texas
21. Sun, W. and Ju, Y., 2015. Multi-timescale and Correlated Dynamic Adaptive Chemistry and Transport Modeling of Flames in n-Heptane/Air Mixtures. In53rd AIAA Aerospace Sciences Meeting (pp. 2015-1382).
22. Sun, W., & Ju, Y. (2015, May). Multi-timescale and correlated dynamic adaptive chemistry and transport (CO-DACT) modeling of flames in jet fuel surrogate mixtures. In 9th US National Combustion Meeting.
23. Sun, W. and Ju, Y., 2016. A Smart CSP Method and Correlated Dynamic Adaptive Chemistry and Transport Algorithm for Computationally Efficient Modeling with A Detailed Mechanism. In 54th AIAA Aerospace Sciences Meeting (p. 1208).

Honors and Awards: May 2015 Distinguished Paper Award of the 35th International Symposium on Combustion, The Combustion Institute
Nov. 2015 Best Paper Award, The Combustion Society of Japan
May 2016 Plenary Lecture, The 52nd Korean Society of Combustion Symposium, Buyeo, Korea.
Dec. 2016 Plenary Lecture, The Fifth International Education Forum on Environment and Energy Science, San Diego, USA.
Jun. 2017 Invited Lecturer, The Bunsen conference, University of Bielefeld, Germany.
July 2017 Distinguished Visiting Fellow, The Royal Academy of Engineering, United Kingdom
Aug. 2017 Honorary Professorship, Xi'an Jiaotong University, China
Oct. 2017 Air Products Distinguished Lecturer, The Pennsylvania State University, USA
Feb.2018 Fellow of the Combustion Institute, The Combustion Institute (international)
Nov. 2018 International Prize, The Japanese Society of Combustion
Nov. 2018 Highly Cited Researcher, Web of Science, Clarivate Analytics.
Jan. 2019 Fellow of School of Engineering, The University of Tokyo.
May 2019 Karl H. Walther Award, THE AMERICAN SCIENTIFIC GLASSBLOWERS SOCIETY.
May 2019 Plenary Lecturer (Selected) for the 38th International Symposium on Combustion, 2020, in Adelaide, Australia; The Combustion Institute (International).

Protocol Activity Status:

Technology Transfer: • The ASURF+ code with CO-DACT algorithm was shared to Combustion Science Engineering Inc. (CSE) for a Navy project on plasma ignition modeling in jet engine.

- The code is used by CSE to calculate the minimum ignition energy and critical ignition radius for plasma ignitors in jet engine.
- Sharing ASURF software for ignition and flame calculations with Argonne National Laboratory. The code is used for engine ignition modeling.
- The cool flame experiments are used for ExxonMobil to characterize their new fuels for advanced gasoline engines.

PARTICIPANTS:

Participant Type: PD/PI
Participant: Yiguang Ju
Person Months Worked: 1.00 **Funding Support:**
Project Contribution:
International Collaboration:
International Travel:
National Academy Member: N
Other Collaborators:

Participant Type: Postdoctoral (scholar, fellow or other postdoctoral position)
Participant: Chao Yan
Person Months Worked: 2.00 **Funding Support:**
Project Contribution:
International Collaboration:
International Travel:
National Academy Member: N
Other Collaborators:

Participant Type: Graduate Student (research assistant)
Participant: weiqi sun
Person Months Worked: 3.00 **Funding Support:**
Project Contribution:
International Collaboration:
International Travel:
National Academy Member: N
Other Collaborators:

Participant Type: Graduate Student (research assistant)
Participant: Tianhan Zhang
Person Months Worked: 10.00 **Funding Support:**
Project Contribution:
International Collaboration:
International Travel:
National Academy Member: N
Other Collaborators:

Participant Type: Graduate Student (research assistant)
Participant: Tianhan Zhang
Person Months Worked: 10.00 **Funding Support:**
Project Contribution:
International Collaboration:
International Travel:
National Academy Member: N
Other Collaborators:

Participant Type: Graduate Student (research assistant)
Participant: Omar Yehia
Person Months Worked: 2.00 **Funding Support:**
Project Contribution:
International Collaboration:
International Travel:
National Academy Member: N
Other Collaborators:

Participant Type: Graduate Student (research assistant)
Participant: Hao Zhao
Person Months Worked: 2.00 **Funding Support:**
Project Contribution:
International Collaboration:
International Travel:
National Academy Member: N
Other Collaborators:

CONFERENCE PAPERS:

Publication Type: Conference Paper or Presentation **Publication Status:** 3-Accepted
Conference Name: The 36th International Symposium on Combustion
Date Received: 31-Aug-2016 Conference Date: 01-Aug-2016 Date Published: 05-Aug-2016
Conference Location: Seoul, Korea
Paper Title: Multi-scale Modeling of Detonation Formation with Concentration and Temperature Gradients in n-Heptane/Air Mixtures
Authors: Tianhan Zhang, Weiqi Sun, Yiguang Ju
Acknowledged Federal Support: **Y**

Publication Type: Conference Paper or Presentation **Publication Status:** 1-Published
Conference Name: 2016 AIAA Science Tech
Date Received: 31-Aug-2016 Conference Date: 04-Jan-2016 Date Published: 08-Jan-2016
Conference Location: San Diego, USA
Paper Title: A Smart CSP Method and Correlated Dynamic Adaptive Chemistry and Transport Algorithm for Computationally Efficient Modeling with A Detailed Mechanism
Authors: Weiqi Sun,Yiguang Ju
Acknowledged Federal Support: **Y**

Publication Type: Conference Paper or Presentation **Publication Status:** 0-Other
Conference Name: The 26th International Colloquium on the Dynamics of Explosions and Reactive Systems (ICDERS)
Date Received: 25-Aug-2017 Conference Date: 01-Aug-2017 Date Published: 28-Jul-2017
Conference Location: Boston
Paper Title: Development of a Multiscale Adaptive Reduced Chemistry Solver (MARCS) for Computationally Efficient Combustion Simulations
Authors: Weiqi Sun, Liang Wang , Temistocle Grenga and Yiguang Ju
Acknowledged Federal Support: **Y**

RPPR Final Report
as of 16-Sep-2019

Publication Type: Conference Paper or Presentation **Publication Status:** 2-Awaiting Publica
Conference Name: Spring Technical Meeting Eastern States Section of the Combustion Institute, March 4-7, 2018 State College, Pennsylvania
Date Received: 05-Sep-2018 Conference Date: 04-Mar-2018 Date Published: 04-Mar-2018
Conference Location: State College, Pennsylvania
Paper Title: Effects of Thermal and Fuel Stratifications and Turbulence Transport on Knocking Formation for Dimethyl Ether/Air Mixtures
Authors: Tianhan Zhang, Weiqi Sun, Liang Wang, Yiguang Ju
Acknowledged Federal Support: **Y**

Summary of Scientific Progress and Accomplishments

Table of Contents

Summary of Scientific Progress and Accomplishments

Statement of the problem studied

Advanced engines need to operate at higher boosted pressure, lower temperature, and variety of alternative fuels for higher energy efficiency, higher power, more fuel flexibility, and less emissions. However, at higher pressures, low temperature chemistry plays a critical role in affecting engine performance, engine knocking, combustion processes, and results in strong turbulence/chemistry interaction as well as new ignition and flame regimes. Quantitative modeling of such complicated reactive flow at extreme conditions requires detailed models for chemical kinetics and transport, and thus is extremely challenging.

Summary of the most important results

In this project, we developed a smart computational singular perturbation (CSP) method and a hybrid multi-timescale and correlated dynamic adaptive chemistry and transport (HMTS/CO-DACT) method for accurate and computationally-efficient modeling of low temperature ignition and knock formation of surrogate diesel fuel mixtures. The results showed that the present CO-DACT method is very computationally efficient to handle detailed chemical kinetics and multi-species transport properties. The method was successfully applied not only to low temperature and high temperature ignition and flame modeling but also to the simulations of engine knocking. The results show clearly that not only low temperature chemistry but also its interaction with turbulence significantly affect knock formation. By considering both the temperature and fuel concentration gradients, an engine knock regime diagram with and without low temperature chemistry is obtained. Furthermore, the CO-DACT method is applied to the modeling of turbulent jet combustion. The results demonstrated that the CO-DACT method enhanced computation efficiency and the results are accurate. Moreover, numerical simulations were applied to the design of a novel inwardly off-center shearing (IOS) jet stirred reactor. The results show that the new IOS jet stirred reactor has an improved distribution of flow residence time. As such, the present study not only provides a computationally efficient tool for engine modeling and fuel design but also advances the understanding of role of low temperature chemistry in knock formation.

1. A multi-timescale and correlated dynamic adaptive chemistry and transport (CO-DACT) method for computationally efficient modeling of jet fuel combustion with detailed chemistry and transport

1.1 Abstract

A correlated dynamic adaptive chemistry and transport (CO-DACT) method is developed to accelerate numerical simulations with detailed chemistry and transport properties in a reactive flow with a jet fuel surrogate. Different sets of phase parameters, which govern the transport properties and chemical reaction pathways, respectively, are proposed to identify the correlated groups for transport properties and reaction pathways in both temporal and spatial coordinates. The correlated transport properties and reduced chemical mechanisms in phase space are dynamically updated by different user-specified threshold values. For the calculation of detailed transport properties, the mixture-averaged diffusion model is employed. For the on-the-fly generation of reduced chemistry, the multi-generation path flux analysis (PFA) method is used. In the present method, the chemical reduction and transport properties calculation are only conducted once for all the computation cells in the same correlated group within the pre-specified thresholds. Therefore, without sacrificing accuracy within the range of uncertainty of mechanisms and transport properties, the CO-DACT

method can eliminate all redundant chemistry reductions and transport properties calculations in temporal and spatial coordinates when the transport properties and chemical reaction pathways are correlated due to the similarities in phase space. The CO-DACT method is further integrated with the hybrid multi-timescale (HMTS) method to achieve efficient integration of chemistry. Simulations of out- ward propagating spherical premixed flames and one dimensional (1D) diffusion ignitions of a jet fuel surrogate mixture, as well as an unsteady spherical propagating diffusion flame of a DME/air mixture are conducted to validate the present algorithm. The impact of the selection of threshold values as well as the dependence of numerical errors on pressure and equivalent ratio are also examined. The results demonstrate that the CO-DACT method can increase the computation efficiency for transport properties by at least two-order of magnitudes. Moreover, it is robust, accurate, and improves the overall computation efficiency involving a large kinetic mechanism. The present results provide insights into knocking mechanisms in engines [1].

1.2 Results and Discussion

In order to validate the HMTS/CO-DACT method, the results and performance of the proposed method are compared against other existing methods, including the VODE, HMTS and HMTS/CO-DAC methods. Detailed comparisons between the implementation of these methods are listed in Table 1. Numerical simulation of unsteady outwardly propagating spherical premixed flames and diffusion ignitions of a jet fuel surrogate mixture are carried out, which cover premixed and non-premixed as well as stretched and un-stretched reactive flow conditions with strong chemistry-transport coupling. Then, the numerical errors of the HMTS/CO-DACT method will be examined with different threshold values, pressures, and equivalence ratios. The mechanism used in this study is comprehensively reduced from a jet fuel surrogate mechanism by using the second-generation PFA method. The surrogate jet fuel consists of four components fuels (40% n-dodecane, 30% iso-octane, 23% n-propyl benzene, and 7% 1,3,5-trimethyl by mole fraction). The reduced mechanism has 425 species and 2275 reactions.

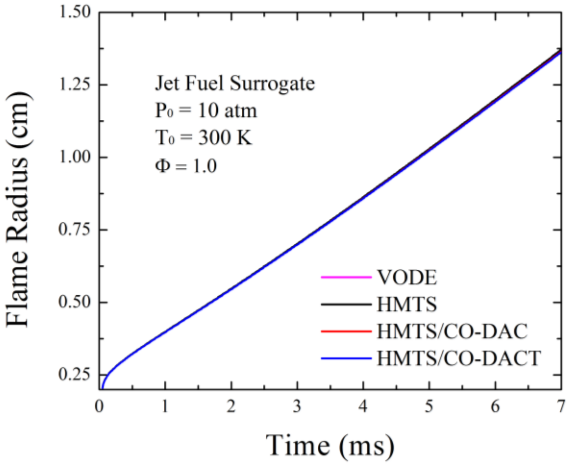

Fig.1 Flame trajectories comparison between VODE, HMTS, HMTS/CO-DAC and HMTS/CO-DACT methods of the stoichiometric jet fuel surrogate mixture at 10 atm and 300 K.

Method	Chemical reduction	Chemical integration	Transport properties
VODE	-	VODE	Mixture-averaged
HMTS	-	HMTS	Mixture-averaged
HMTS/CO-DAC	Correlated PFA	HMTS	Mixture-averaged
HMTS/CO-DACT	Correlated PFA	HMTS	Correlated mixture-averaged

Table 1. Comparisons of details between different methods [1].

1.2.1 Premixed outwardly propagating spherical flames

The premixed spherical propagating flame is ignited by a hot spot with 2000 K and 2 mm in radius at the center (X=0 cm) of the spherical coordinate. The homogeneous stoichiometric jet fuel surrogate mixture has the initial conditions with 10 atm and 300 K. The overall size of the computation domain is 5 cm and the boundary conditions are reflective at x = 0 and transmissive at X = 5 cm. The results of flame trajectory are compared between the VODE, HMTS, HMTS/CO-DAC and HMTS/CO-DACT methods in Fig.1. The results demonstrate an excellent agreement between these methods. The maximum relative error along the flame trajectory among all these methods is less than 0.5%, which is much smaller than the experimental uncertainty of transport properties and flame speed measurements for chemistry validation (~5%).

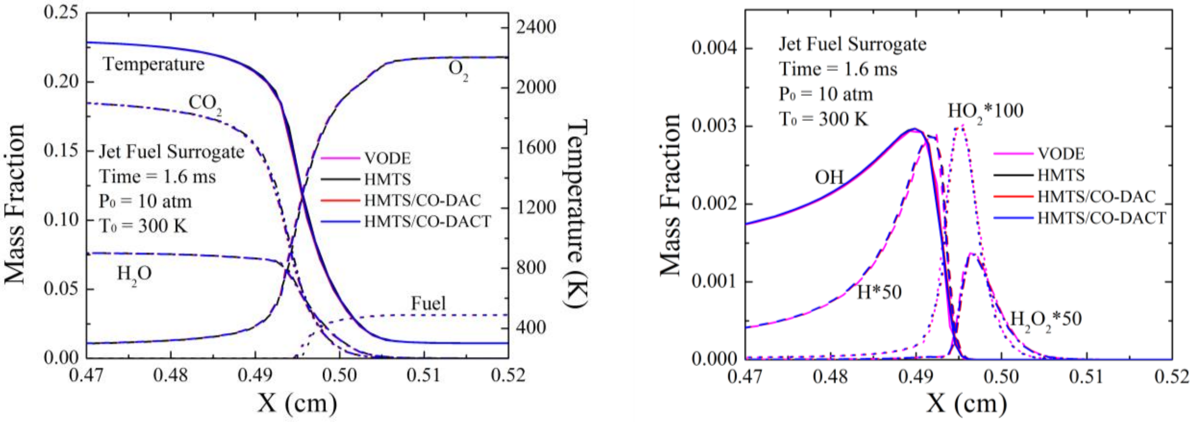

Fig. 2a (left) Distributions of temperature and major species (O2, Fuel, H2O and CO2) in the stoichiometric premixed flame at 1.6 ms**; 2b (right):** Distributions of minor radicals (OH, H, HO_2 and H_2O_2) in the stoichiometric premixed flame at 1.6 ms.

Figures. 2a and 2b plot the spatial distributions of selected phase parameters, including temperature, O_2, Fuel, H_2O and CO_2, at physical time t = 1.6 ms. The flame surface is located around the location X = 0.495 cm. The results in Fig.2a demonstrate that the HMTS/CO-DACT method is accurate enough to capture the major structure of a premixed flame, including temperature and major species. The mass fraction distributions of the selected minor species and radicals, including OH, H, HO2 and H2O2, at the same physical time t = 1.6 ms, are plotted in Fig. 2b to examine and demonstrate the accuracy of the HMTS/CO-DACT method on capturing those species which are not tracked and included in the phase space. Fig.2b also shows that the minor species follow the same accuracy as the major species and the discrepancies between different methods are negligible. Therefore, it successfully demonstrates that the proposed HMTS/CO-DACT method can accurately predict the distributions of minor species and radicals for a large jet surrogate fuel mixture.

Figure 3a shows the comparisons of the CPU time consumed by the transport properties calculation between different methods. The purple, black and red lines, which represent the VODE, HMTS and HMTS/CO-DAC methods, respectively, overlap together because the transport properties in these methods are computed by the same mixture-averaged diffusion model, as shown in Table 1. Thus, the CPU time of transport properties in first three methods should be the same. By comparing the HMTS/CO-DACT method with other methods, it shows that the proposed CO-DACT method (blue line) is 230 times faster than the transport properties calculation in the mixture-averaged model, which is a dramatic increase of the computation efficiency for a large kinetic mechanism. Figure 3b is the overall CPU time comparisons between VODE, HMTS, HMTS/CO-DAC and HMTS/CO-DACT methods at physical time *t* = 1.6 ms. The green, purple and red sections represent the CPU time consumed by convection flux, diffusion flux and transport properties calculation, respectively, and the blue section is the computation time of the chemical integrations. It is seen from this figure that compared to the first three columns, the proposed HMTS/CO-DACT method can significantly reduce the computation cost of transport properties calculation and, most important, makes it negligible even when a large chemical mechanism with several hundreds of species is involved. With the present CO-DACT method, the overall computation for flame propagation can be accelerated by factor of three compared with the original HMTS method and becomes more than one order of magnitude faster than the VODE method.

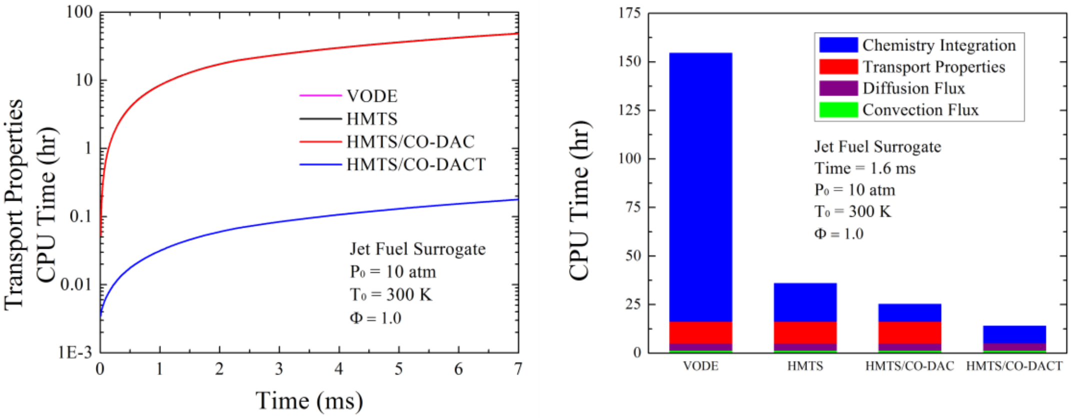

Fig. 3a (left) Comparison of CPU time for the transport properties calculation between VODE, HMTS, HMTS/CO-DAC and HMTS/CO-DACT methods of the stoichiometric premixed flame. **3b (right)**: CPU time comparison between VODE, HMTS, HMTS/CO-DAC and HMTS/CO-DACT methods at 1.6 ms of the stoichiometric premixed flame.

1.2.2 Diffusion ignition and cool flames

The diffusion ignition is initiated at 1 atm and 1200 K with the pure air in the left half domain and pure fuel in the right half domain. A planar 1D domain with 5 cm is used and the reflective boundary conditions are applied for both side. The results of the diffusion ignition are compared

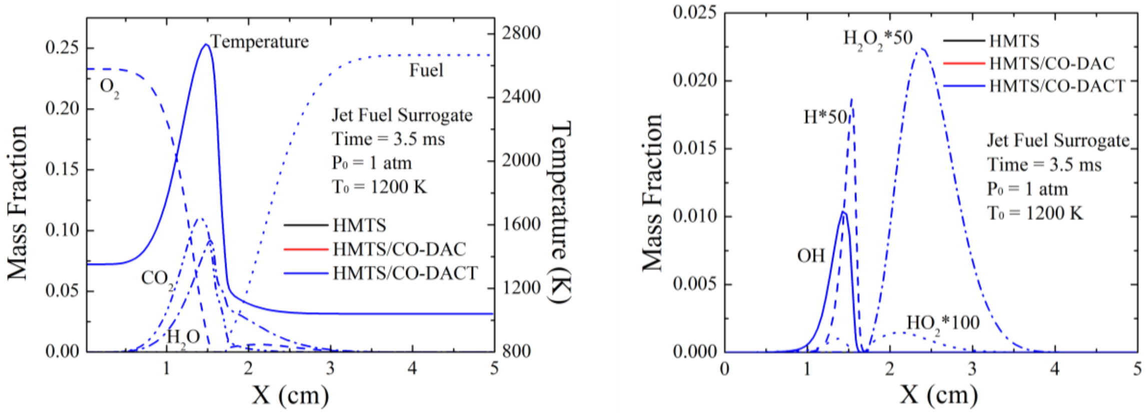

Figure 4a (left): Distributions of temperature and major species (O_2, Fuel, H_2O and CO_2) in the diffusion ignition at 3.5 ms. **4b (right):** Distributions of minor radicals (OH, H, HO_2 and H_2O_2) in the diffusion ignition at 3.5 ms.

between HMTS, HMTS/CO-DAC and HMTS/CO-DACT methods. Figures 4a and 4b, respectively, show the distributions of temperature, stable and radical species such as O_2, Fuel, H_2O and CO_2, H, H, HO_2 and H_2O_2, at $t = 3.5$ ms. Once again, it shows an excellent agreement. Fig.5 shows that the HMTS/CO-DACT methods is 200 times faster than the other methods.

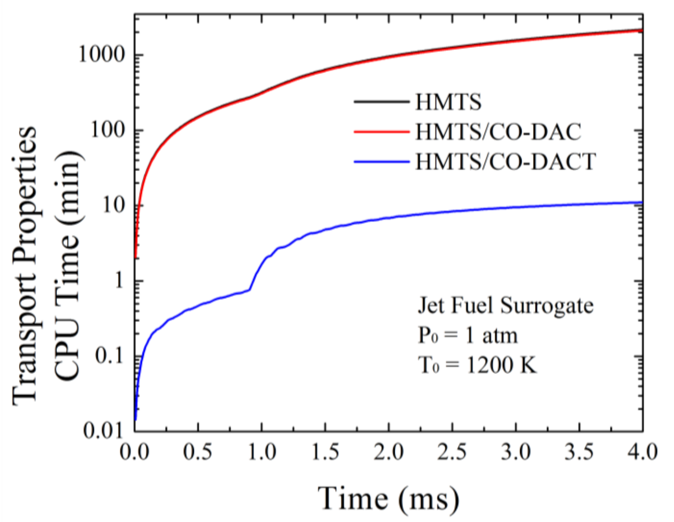

Figure 5: Comparison of CPU time for the transport properties calculation between HMTS, HMTS/CO-DAC and HMTS/CO-DACT methods of the diffusion ignition.

To further validate the CO-DACT method for unsteady ignition including cool flame formation, a numerical study of transient combustion involving fuel injection into a hot air in a spherical chamber is conducted. The numerical configuration is shown in Fig. 6a. The spherical chamber is 20 cm in diameter with an adiabatic wall boundary condition. At the center of the chamber, there is a porous sphere with 2 cm in diameter allowing fuel injection into the chamber. Initially, the gas in the chamber is pure air at 20 atm and 700 K and quiescent. At time $t = 0$, be injected into the chamber from the porous sphere surface with an injection speed fixed at $U_0 = 1$ m/s. The inlet fuel mixture contains 10% DME and 90% N_2 in mole fraction. The boundary condition of the out wall is adiabatic and reflective. Fig. 6b plots the comparisons of the predicted time histories of the maximum temperatures (solid lines) and the corresponding locations of the maximum temperature (dash lines) of the unsteady ignition and flame formation process. The black, red and blue lines are the results calculated by HMTS, HMTS/CO-DAC and HMTS/CO-DACT methods, respectively. Due to the high pressure and

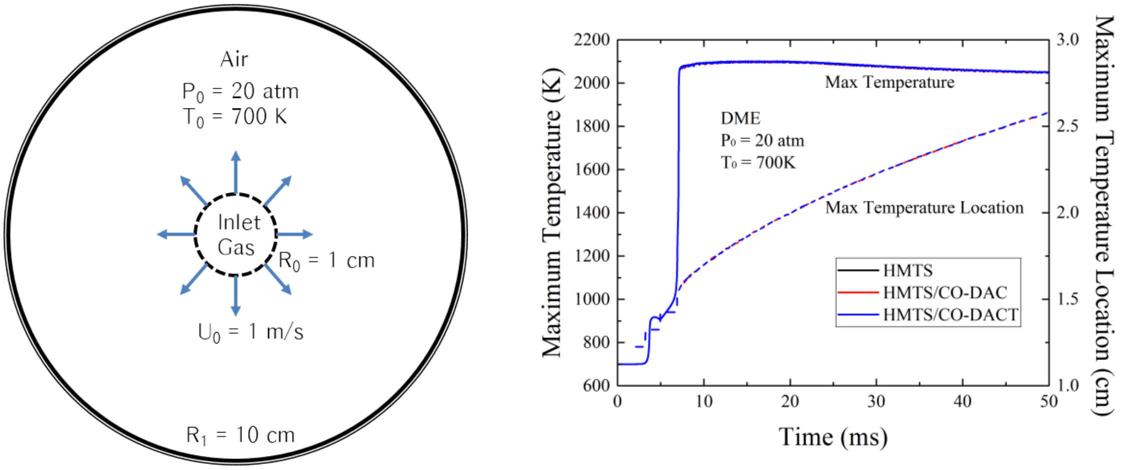

Fig.6. (a) (left): Schematic of the unsteady ignition and flame formation in a spherical diffusion flame configuration. **(b) (right):** Comparisons of the predicted time history of the maximum temperatures and corresponding locations between HMTS, HMTS/CO-DAC and HMTS/CO-DACT methods of unsteady diffusion ignition/flame formation.

elevated temperature, a two-stage auto-ignition and the cool diffusion flame formation can be observed clearly in Fig.6b. The low temperature ignition happened around 4 ms. Then, a cool diffusion flame is induced with temperature at 910 K. The cool flame lasted for 3 ms. After that, a hot ignition occurred at 7 ms and the cool flame became a hot diffusion flame and propagates outwardly. Note that the ignition, cool flame formation, and cool flame to hot flame transition processes in the simulated configuration are strongly governed by molecular diffusion and are not in quasi-steady state. This figure demonstrates clearly that the proposed CO-DACT method together with HMTS method can accurately capture the maximum temperature and the corresponding locations for both high temperature and low temperature ignition and diffusion flames. The maximum relative error between HMTS and HMTS/CO-DAC is less than 1%.

1.3 Conclusion

A correlated dynamic adaptive chemistry and transport (CO-DACT) method is developed and integrated with the hybrid multi-time scale (HMTS) method to drastically accelerate the calculation of transport properties and chemistry in an unsteady reactive flow with detailed chemical kinetics and transport. In this method, the correlated groups in temporal and spatial coordinates for both transport and chemistry are identified successfully by applying two different sets of phase parameters, which govern, respectively, transport properties and chemical reaction pathways. The proposed CO-DACT method is demonstrated, mathematically and numerically, to be first-order accurate and the numerical errors in transport properties are on the order of the user-specified threshold value for discretizing the phase space. The CO-DACT method can be extended to 2nd order accuracy with a linear extrapolation of the transport properties. Validations in outward propagating spherical premixed flames, diffusion ignitions and spherical propagating diffusion flames illustrate that the proposed HMTS/CO-DACT method can accurately reproduce flame speed, ignition delay time, flame structure, and species distributions. Moreover, the calculation of transport properties in the CO-DACT method is 200 times faster than the mixture-averaged method. Numerical simulations with different threshold values, pressures, and equivalence ratios show that the method is rigorous in a very broad range. Therefore, the present HMTS/CO-DACT method provides an innovative and computationally efficient way for DNS of combustion modeling with large chemical kinetics and detailed transport properties.

2. Development of HMTS/CO-DACT method and adaptive time-step matching G-scheme for efficient computational modeling

2.1 Abstract

To develop a multiscale adaptive reduced chemistry solver (MARCS) for computationally efficient modeling of a reactive flow, the Hybrid Multi-Timescale (HMTS) method and G-Scheme have been evaluated and compared for both homogeneous auto-ignition and 1-D premixed spherical propagating flame calculations with detailed chemical kinetics of hydrogen, methane, dimethyl ether, and n-heptane. It is demonstrated that the CPU time of HMTS and G-Scheme methods depends on the number of species of the kinetic mechanisms, respectively, linearly and to the third power. For ignition, the results show that the G-Scheme method is faster than HMTS method when the species number of the chemical mechanism is below 40. The CPU Time of G-Scheme increases dramatically when the number of species of the detailed mechanisms is increased due to the huge computation cost of matrix inversion and reaction mode decomposition. Specifically, the G-Scheme method is faster at the induction stage of ignition and the near-

equilibrium condition after ignition due to the large integration time step determined by the method adaptively. The HMTS method is faster at near the ignition point and for a large kinetic mechanism due to the fast convergence at a small base time step. A new concept of adaptive time-step matching of G-scheme with CO-DACT is proposed and preliminarily tested. The present results suggest that it is possible an MARCS for computationally efficient modeling of combustion by adaptively taking the advantages of the computation efficiency of the HMTS method and the G-Scheme in different local combustion regimes and reduced mechanism sizes and integrating with the co-related dynamic adaptive chemistry and transport method (CO-DACT).

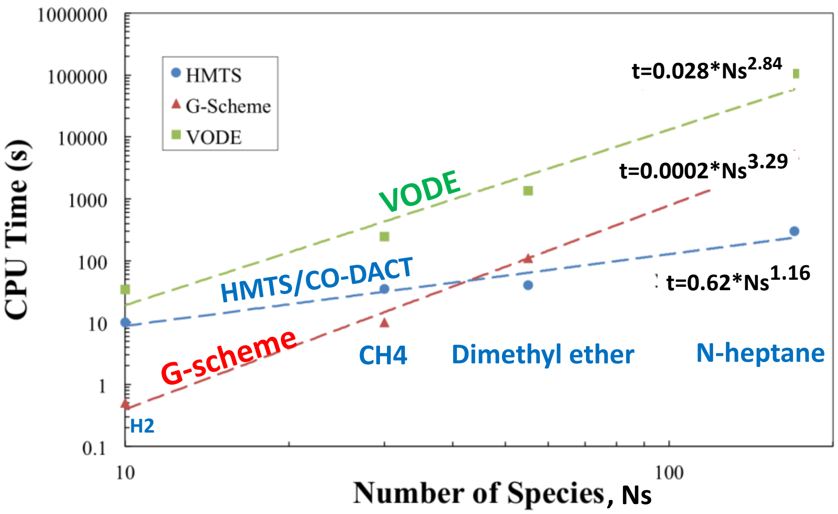

Fig. 7. Dependency of total CPU time on the number of species calculated by HMTS method (blue), G-Scheme (red) and VODE method (green) for the homogenous auto-ignition process.

2.2 Results and discussions

The computation efficiencies of HTMS, G-Scheme, and VODE are examined and compared in this study for four different mechanisms of H2, CH4, dimethyl ether, and n-heptane, having number of species, respectively, from 10, 30, 55 to 170, for homogenous ignition and flame propagation. Figure 7 are plotted the comparisons for three different methods: HTMS (blue), G-Scheme (red) and VODE (green), for auto-ignition. The exponential fittings for these three methods are also shown on this figure as the dash lines. It demonstrate that the computation cost of HMTS method is linearly dependent on the size of mechanism since the species equations in HMTS method is decoupled and integrated separately and the CPU time is proportional to the number of equations. On the other hand, the CPU time of G-Scheme and VODE method are proportional to the cubic of the mechanism size, due to the matrix operations are involved. For the small mechanism, G-Scheme is faster than HMTS by taking the advantage of the large integration time steps. However, when the size of mechanism is getting larger, G-Scheme becomes slower than HMTS method because the slow integration for a single step. The intersection of HMTS and G-Scheme method on Figure 7 is corresponding to 41 species. Therefore, it provides a possible strategy to combine these two methods together: when the size of the local mechanism is below 41, G-Scheme would be applied to take the advantage of the large integration time steps; while the mechanism is larger than 41, HMTS method would be used to gain the fast integration of a single time step. The G-Scheme could be used, for large mechanism, at very early ignition stage and near-equilibrium where it is still faster than other methods.

In order to use the G-scheme for efficient modeling in flames, we need to develop an adaptive time step matching method for reaction and diffusion. The schematic of the concept of adaptive time step matching method in flame calculations is shown in Fig.8. The *x* axis represents the space coordinate, *x*, and the y axis the integration time, *t*. For three computation cells, x_1, x_2 and x_3, which represent the near-equilibrium region, flame surface and unburned region, respectively, their cell sizes are different because the adaptive grid is applied and the smallest cell, x_2, is located on flame surface. The integration starts from time step t^0. The convection and diffusion fluxes are computed and integrated at every time step Δt_{base}, which is determined by the smallest grid size and CFL number. Thus, these three cells use the same time step to conduct the transport flux integration, which guarantee the mass conservation in the calculation. The chemical integration time steps, τ, in G-Scheme are determined locally and they are represented by the orange dash line in Fig.8. Three cells, x_1, x_2 and x_3, have different chemistry time steps, τ_1, τ_2, and τ_3 due to the different local thermodynamic states. The chemistry time step in the second cell is the smallest because on the flame surface, the reactions are intensive and the characteristic time is smaller than the time scale of transport terms, Δt_{base}. Therefore, in cell x_2, several G-Scheme integrations (2 in this case) are conducted within one transport integration. This method has been tested for hydrogen and methane mechanism, the preliminary results showed this adaptive time step matching method can accelerate computation time significantly. Future studies will integrate this method with HMTS and G-scheme dynamically.

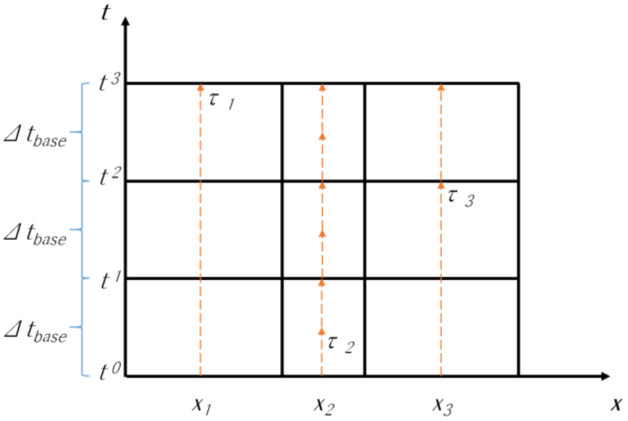

Fig.8. Schematic of the adaptive time step matching method.

3. The smart CSP method

3.1 Mathematical formulation

Considering a reaction system with *N* species and *R* reactions, the system can be represented by an *N+1* dimensional composition space constructed by the concentration of species and temperature *T*. Each state of the reaction system is a point, $\mathbf{y}$, in the composition space. The variation of the state $\mathbf{y}$ can be described by the following ODE system:

$$\frac{d\mathbf{y}}{dt} = \mathbf{g}(\mathbf{y}), \tag{1}$$

where *t* is time and $\mathbf{g}$ is the reaction rates vector. Each reaction makes a contribution to the reaction vector:

$$\mathbf{g}(\mathbf{y}) = \sum_{r=1}^{R} \boldsymbol{\alpha}_r \Omega^r(\mathbf{y}). \tag{2}$$

$\boldsymbol{\alpha}_r$ is the stoichiometric coefficient column vector and $\boldsymbol{\Omega}^r$ is the *r*-th net reaction rate.

In the simple computational singular perturbation (CSP) method, the fast reaction rates (1-*M*th reactions) can be represented by using the slow reaction rates *(M+1* to *R* reactions) using the following representation,

$$\Omega_{\infty}^{m'} \equiv -\sum_{k=1}^{R-M}\left(\sum_{m=1}^{M}\Theta_{m}^{m'}\Gamma_{M+k}^{m}\right)\Omega^{M+k}. \tag{3}$$

Multiplying Eq. (3) on its left by the matrix $\Theta_m^{m''}\tau^m$ and summing over all *m*, we obtain the following equations:

$$\Omega^{m''} = \Omega_\infty^{m''} + \omega_{fast}^{m''}, \qquad m''=1,....,M, \tag{4}$$

where

$$\omega_{fast}^{m''} \equiv \sum_{m=1}^{M} \Theta_m^{m''}\tau^m \frac{d\Omega^m}{dt}. \tag{5}$$

Equation (5) is the analytical solution of the fast reaction rate, $\Omega^{m''}$, represented by the combination of slow reaction rates, $\Omega_\infty^{m''}$, and fast exhaust term $\omega_{fast}^{m''}$. All the τ^m are negative and small, thus the fast Ω^m are expected to rapidly decay toward the slower evolving Ω_∞^m. After the initial transient, the ω_{fast}^m term on the right hand side of Eq. (4) is expected to be a small 'correction' term. By using Ω_∞^m, which only contains the slow reaction rates and is not stiff, to replace the stiff Ω^m, stiffness in the ODE system can be removed and the computation cost of the chemical integration can be dramatically reduced.

Even though the simple CSP method has a promising performance to solve the stiff ODE system, there are still several practical difficulties that prevent it to be implemented in the real simulations: The first difficulty is the calculation of characteristic time τ^r in the large chemical systems; and the second difficulty is the singularity of the matrix $\Gamma_{m'}^m$, which does not have inversion for $\Theta_{m'}^m$ and causes the invalid derivations of the CSP formulations. In order to overcome these difficulties and make the simple CSP method available in the real implementations, we propose a Smart CSP (S-CSP) method by analytically solving the characteristic times and forming a pre-generated library to eliminate the singularity in matrix, $\Gamma_{m'}^m$. In the S-CSP, at first, an analytical expression of the characteristic time τ^m in Eq.(5) is developed. In addition, in order to remove the singularity in matrix $\Gamma_{m'}^m$ in Eq.(3), we must eliminate the linearly dependent reactions in the fast reaction subspace. So the fast reactions should not be only determined by the characteristic time but also determined by the correlations of the reactions. However, it is time consuming to check whether all the selected fast reactions are linearly independent during the run time, especially when the number of the fast reactions is large. Fortunately, the directions of reactions are only determined by the column vector, $\boldsymbol{\alpha}_r$, which is a non-dimensional constant and does not change with time. Therefore, it is possible to check the dependence of the reactions before the calculation. Based on this idea, in our S-CSP method we propose a pre-generated library that contains all the linearly independent reactions. We rank all the reactions by their characteristic times from pre-calculations, such as auto-ignition and flame-speed calculations, and add the reactions to the library from fast to slow. If one reaction is linearly dependent on the existing reactions in the library, we skip it and continuously add the next one, until the number of the reactions in the library is the same as the freedom in the system, $N+1-E$. Then during the real simulation, the fast reactions is first identified by the characteristic times, but we only place those fast reactions that included in the pre-generated library to the fast subspace to form the matrix $\Gamma_{m'}^m$. By doing this, we can avoid the singularity in the matrix. After updating the fast reaction rates by the combination of slow reactions, the implicit integration method is used to solve the ODE system.

3.2 Results and Discussion

The homogenous auto-ignition process of the stoichiometric H_2/air mixture is conducted at 10.0 atm and different temperatures. The characteristic time of reactions in the system will be examined first, followed by the comparisons of ignition delay time and CPU time between the S-CSP method and HMTS method. The integration time step Δt in this study is 10^{-8} s and the safe parameter to determine the fast species is 10. Thus, if the characteristic time of a reaction is smaller than $10\Delta t = 10^{-7}$ s, this reaction will be considered as fast.

Figure 9 shows the characteristic time distributions at three time events in the ignition process. The red, yellow and blue columns are the distributions, respectively, at reaction initiation (t = 7 μs), the onset of ignition (t = 543 μs) and the equilibrium state (t = 896 μs). It is seen that the distribution of the characteristic time shift to the small timescale in the ignition process. Moreover, the smallest time scale among all these three distributions only contains 2 reactions. Therefore, this figure demonstrates that even if only the top 2 fastest reactions are removed in the system, the stiffness can still be reduced by at least one order of magnitude.

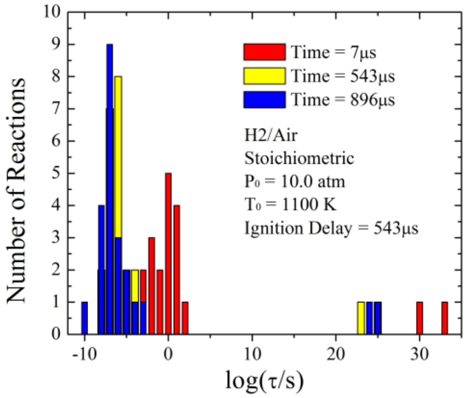

Fig. 9 The distribution of characteristic reaction time, respectively, at: (1) beginning of the process (red); (2) onset of ignition (yellow); (3) the equilibrium state (blue).

Figure 10 shows the ignition delay time comparisons between the S-CSP method and HMTS method at 10.0 atm and different temperatures. Since hydrogen is a simple molecule and doesn't have long hydro-carbon chains, there is no low temperature chemistry in the system and therefore the ignition delay time monotonically increases with the decreasing of the temperature. It is seen from Fig.10 that the agreement between the S-CSP method and the HMTS method is excellent and the maximal relative error in ignition delay time is 3.4%. Therefore, it proved the accuracy of the S-CSP method. In order to examine the computation efficiency of the S-CSP method, the CPU times of the S-CSP method and the HMTS method are compared. The results show that due to stiffness removal of in the current S-CSP method can improve the computation efficiency by one order of magnitude by increasing the integration time-step, thus dramatically increases the computation speed.

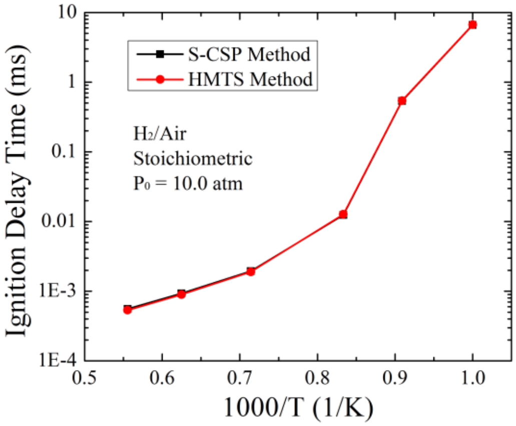

Fig. 10 Ignition delay time comparisons between the S-CSP method and HMTS method with homogeneous H2/Air mixture initiated at 10.0 atm.

3.3 Conclusion

A Smart CSP (S-CSP) method is developed to remove the stiffness of the ODE system automatically without human experience. The present method enables the implementation of the simple CSP method by eliminating the linearly dependent reactions in the fast reaction subspace and introducing an analytical formulation of the characteristic time of elementary reactions. The correlated dynamic adaptive chemistry and transport (CO-DACT) method is integrated with the S-CSP method to provide the local reduced chemical kinetics and transport coefficients. With the current simple implementation, which only removes the top 2 fastest reactions, the S-CSP method has shown its accuracy and demonstrated the ability to reduce the stiffness in the system by one order of magnitude. Therefore, with the further developed library for the linearly independent fast reactions, the S-CSP method has a great potential to accelerate the chemical integration with large detailed chemical kinetics.

4. Multi-scale Modeling of Detonation Formation with Concentration and Temperature Gradients in n-Heptane/Air Mixtures

4.1 Abstract

Detonation/knocking initiation and ignition wave propagation in concentration stratified n-heptane/air mixtures with and without temperature gradient are numerically modeled by using the correlated adaptive chemistry and transport (CO-DACT) method coupled with the hybrid multi-timescale (HMTS) method in a one-dimensional planar constant volume chamber. For concentration gradient only, three combustion modes, including spontaneous ignition, detonation to spontaneous ignition transition, and a fully developed detonation mode, are observed corresponding to low, critical, and high concentration gradients, respectively. It is shown that the onset boundary of the three combustion modes are strongly affected by the coupling between concentration and temperature gradients. It is found that at a given concentration gradient, the temperature gradient can either promote or inhibit the detonation formations, depending on the variation of the associated ignition delay times. A comprehensive criterion for the onset of different combustion models involving both concentration and temperature gradients is presented and verified numerically. The results show that the critical concentration gradient for detonation initiation is greatly modified by the existence of a temperature gradient and vice versa. The present results provide insights into knocking mechanisms in engines [2].

4.2 Numerical model

Engine knocking often occurs near the wall where there is a high fuel concentration gradient due to the vaporization of droplets impinged on the wall. To model the effect of concentration gradient on knocking and detonation formation, we simplify the problem to a one-dimensional ignition and detonation initiation process in a constant volume chamber with a concentration gradient with and without temperature gradient on the left boundary of the domain.

N-heptane is used as the fuel in the simulations since it is one of the major components of the Primary Reference Fuel (PRF) and exhibits rich low temperature reactivity in the NTC region. A comprehensively reduced n-heptane kinetic model (170 species and 962 reactions) produced by the multi-generation path flux analysis (PFA) method is applied. The domain size is 3 cm with reflective boundary conditions on both sides. The ambient mixture is stoichiometric and the initial pressure is 40 atm to represent a typical working condition in a gasoline engine. A concentration gradient is created on the left boundary with the size of 3 mm to mimic a near-wall stratified fuel mixture. To understand the coupling effect of concentration and temperature gradient on the combustion modes, different temperature gradients are also imposed in the domain. In order to conduct the simulations efficiently with a large chemical kinetic model, the correlated dynamic adaptive chemistry and transport (CO-DACT) method coupled with the hybrid multi-timescale

(HMTS) method is applied. Specifically, the correlated reduced mechanisms and correlated transport properties are updated dynamically by using the CO-DACT method. Then, the HMTS method is used to integrate the chemical reactions based on the local reduced mechanisms. To maintain an adequate spatial resolution, a multi-level dynamically adaptive mesh refinement is conducted by using adaptive simulation of unsteady reactive flow (ASURF+) code[4]. The smallest cell in this study is 8μm and the corresponding integration time step is 0.8 ns. To achieve high resolution computational fidelity and to capture the sharp discontinuity on the detonation front, a third-order weighted essentially non-oscillatory (WENO) scheme is employed to integrate the convection fluxes. The integration of ASURF+ code with HMTS/CO-DACT and WENO scheme has been extensively validated in our previous studies.

4.3 Coupling effects of temperature and concentration gradients on detonation formation

In practical applications, due to the inevitable fluctuations in engines, the concentration gradient and temperature gradient often appear simultaneously. Thus, it is necessary to investigate the combined effect of temperature and concentration gradients on the detonation initiation.

In order to analyze the concentration and temperature gradient coupling, we conducted simulations with both concentration and temperature gradients. The distribution of the temperature with a given temperature gradient, is shown in the following equations:

$$T = \begin{cases} T_0 + (0.3 - x)(-\nabla T) & x < 0.3cm \\ T_0 & x \geq 0.3cm \end{cases} \tag{6}$$

Fig. 11 (a) and (b) show the comparisons of the ignition modes calculated at same normalized concentration gradient ($\xi_\varphi = 0.3$) without and with normalized temperature gradient ($\xi_T = 10$), at initial temperature and pressure of 800 K and 40 atm. The comparison clearly shows that without temperature gradient (Fig.11a), there is only spontaneous auto-ignition. However, with the small temperature gradient (11b), a denotation wave is formed immediately after the onset of ignition on the left boundary of the domain. Therefore, Figs.11a and 11b clearly demonstrate that the temperature gradient can significantly promote the formation of detonation together with a concentration gradient.

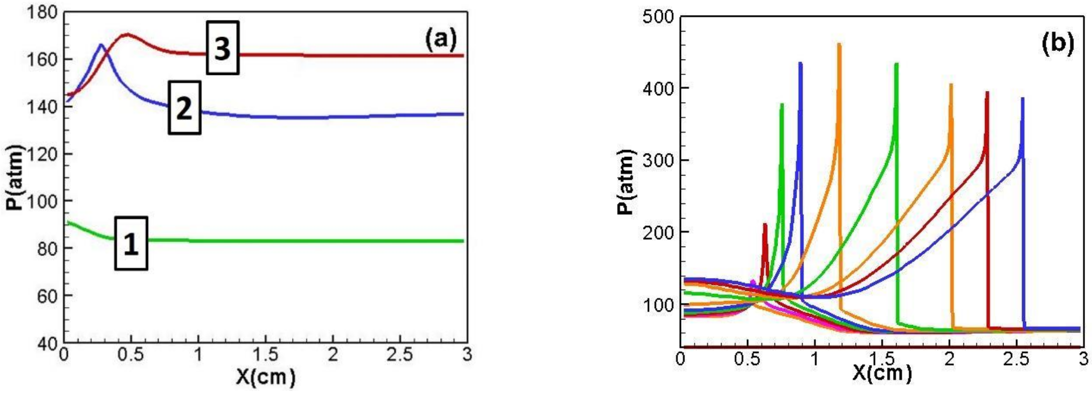

Fig. 11 (a) Temporal evolution of pressure for T_0=800K, P_0=40atm, ξ_φ=0.3, ξ_T=0. The time sequence is 1:845μs, 2:846μs, 3:847μs. (b) Temporal evolution of pressure for T_0=800K, P_0=40atm, ξ_φ=0.3, ξ_T=10.

4.4 Critical conditions for detonation formation with concentration and temperature gradients

In order to answer the question of why the temperature gradient can have different influences on the detonation formation and to gain a deeper understanding of the concentration and temperature gradient coupling, we conduct a first order Taylor expansion of the ignition delay time to define a new normalized critical gradient on the temperature and concentration phase space by using:

$$C_{T\phi} = a^{-1}\left(\frac{d\tau(T,\phi)}{dx}\right)^{-1} = a^{-1}\left(\frac{\partial\tau}{\partial T}\frac{\partial T}{\partial x} + \frac{\partial\tau}{\partial\phi}\frac{\partial\phi}{\partial x}\right)^{-1} \tag{7}$$

If the normalized critical gradient is smaller than unity, the supersonic ignition wave front will be formed in the domain and the reaction front is governed by spontaneous ignition. If the normalized critical gradient is larger than unity, the chemical heat release is able to couple with the pressure wave and form a detonation. Thus, we define $C_{T\Phi}=1$ as the critical boundary to separate the spontaneous ignition mode from the detonation mode. This proposed detonation boundary in Eq. (7) is numerically verified by using different combined concentration and temperature gradients and the results are plotted in Fig.12.

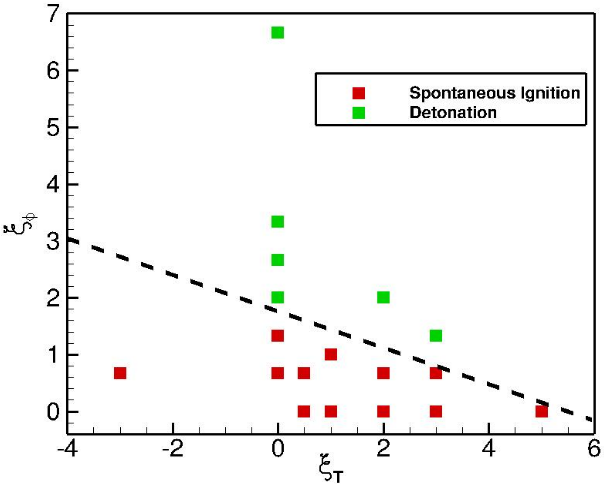

Fig. 12 Different ignition modes under the coupling of temperature and concentration gradients for T=900K, ϕ=1 in the outer region.

4.5 Conclusions

The effect of initial concentration gradient and temperature gradient on the different ignition modes and detonation formation are investigated. The results show that both concentration gradient and its combination with temperature gradient have significant impact on detonation initiation. It is found that with concentration gradient only, there are three combustion modes: 1) a supersonic spontaneous auto-ignition mode with the concentration gradient smaller than the critical value, 2) a detonation to spontaneous auto-ignition transition mode when the initial concentration gradient is close to the critical concentration gradient, and 3) a fully developed detonation mode with the concentration gradient greater than the critical value. Moreover, the results show that the temperature gradient is strongly coupled with concentration gradient to affect the combustion modes. Depending on the mixture composition, at the same concentration gradient, the appearance of temperature gradient can either promote or inhibit the detonation formation. A normalized critical gradient involving both temperature and concentration gradients is proposed by using the first order Taylor expansion of ignition delay time. A general criterion for the onset of detonation initiation involving both concentration and temperature gradients is presented. Numerical simulations of detonation formation with various combined concentration and temperature gradients confirmed that the proposed critical criterion is rigorous. The present study provides insights into the effect of concentration gradient on detonation formations and extends the understanding of knocking formation in advanced engines with simultaneous thermal and concentration gradients.

5 The effects of low temperature chemistry and turbulent transport on knocking formation

5.1 Abstract

The laminar flame speeds and structures of near-limit autoignition-assisted cool and warm n-heptane/air flames at different ignition Damköhler numbers which is the ratio between flow residence time and the ignition delay time, elevated temperatures and pressures are studied computationally and analytically over a broad range of equivalence ratios. The primary objective of this work is to understand the effects of ignition Damköhler number, mixture temperature, equivalence ratio, and pressure on the dynamics and structures of cool and warm flame propagation near the flammability limit. Different transitions among near-limit cool, warm, and hot flames are examined. The results show that both cool and warm flame structures and propagation speeds change dramatically with the increase of the ignition Damköhler number. Moreover, the dependence of normalized cool and warm flame speeds on the ignition Damköhler number is affected by the equivalence ratio, pressure, and flame regimes. Furthermore, for equivalence ratios within the hot flame flammability limits, the results show that there exist two flame speeds, one for the hot flame and the other for the cool flame. It is shown that the cool flame speed has a non-monotonic dependence on the initial mixture temperature due to the negative temperature coefficient (NTC) effect. However, the warm flame speed has a much weaker NTC effect and the hot flame speed only depends monotonically with the increase of the initial temperature. The results also reveal that the lean cool flame speed can be much higher than the hot flame speed near the NTC region. Finally, a simple analytical model for predicting the flame speed of autoignition assisted flames is developed. The model implies that the reduced activation energy of autoignition strongly affects the flame speed dependence on ignition Damköhler number. The present results significantly advanced the understanding of near-limit low temperature flame dynamics [3].

5.2 Results and Discussion

Fig. 13a shows the comparison of detonation peninsula with and without low temperature chemistry by using the normalized temperature and concentration gradient, ξ, and the normalized heat release time, ε. The results show that the critical boundary of detonation peninsula with and without low temperature chemistry is the same. The result clearly reveals that the super knock or detonation formation requires a large heat release rate from the hot ignition. Low temperature ignition alone does not control the onset conditions of knocking. The reason for this is because knocking is an outcome of direct coupling between shock wave and ignition. The shock wave created by the heat release rate of low temperature ignition is not strong enough to cause auto-ignition. Therefore, the mixture has to have enough chemical energy so that the hot ignition will create a strong shock wave and enable the coupling between ignition and shockwave and results in detonation or knocking.

Fig.13b shows the same detonation peninsula of Fig.13a, but the concentration and temperature gradients ξ* is now normalized by the same ignition delay time with low temperature chemistry. It is clearly seen that the low temperature chemistry can either enhance or suppress detonation occurrence depending on the mixture conditions. Therefore, to avoid engine knock, both engine operation conditions and fuel design are important.

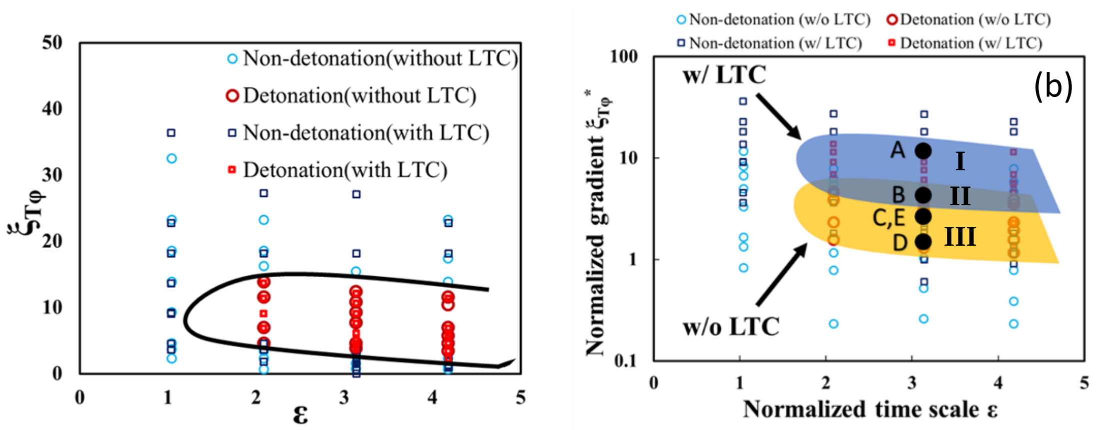

Fig.13 a (left): Detonation (red square) peninsula of dimethyl ether/air mixtures with normalized concentration and temperature gradients (ξ) and heat release rate (ε) using the mechanisms with and without low temperature chemistry. b (right): Detonation peninsula with normalized concentration and temperature gradients ξ* normalized by the same ignition delay time with low temperature chemistry and heat release rate (ε) using the mechanisms with (blue) and without (green) low temperature chemistry.

To understand how low temperature ignition affect knocking formation, Fig.14 shows the comparison of the time history of ignition to detonation transition with and without low temperature chemistry at the same ignition temperature and concentration gradients. It is seen that the low temperature chemistry significantly advanced the occurrence of detonation (knocking). It is seen that the heat release rate by low temperature ignition dramatically accelerated the occurrence of hot ignition and enhanced the coupling between ignition and shock wave. Therefore, although low temperature ignition does not change the mixture compositions of the detonation boundary, it can significantly enhance and accelerate the knocking formation. As such, the low temperature ignition properties of a fuel will dominate the low speed pre-ignition in engines and the occurrence of super-knock.

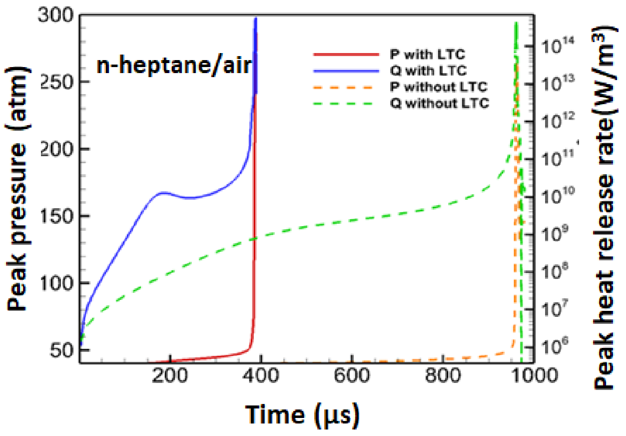

Fig.14 Comparison of time histories of peak pressure and peak chemical heat release rate with and without low temperature chemistry (LTC)

The ignition transition to detonation will also be affected by turbulent transport. In this studies, different turbulent flow properties (Table 1) were used to examine the impact of turbulent transport on knocking formation in a two-dimensional (2D) turbulent flow. Fig. 15 shows the comparison of temperature and pressure distributions between Case 1 and Case 2 (Table 1) with different turbulent eddy timescales at two time steps, respectively, for initial stage of ignition. At t=385μs, the ignition kernel size of Case 2 (longer turbulent eddy timescale) is much larger than Case 1 (shorter turbulent eddy timescale). Moreover, the detonation transition time and detonation peak pressure for Case 2 are also longer and lower, respectively, than those of Case I. Therefore, from these simulations, we can conclude that turbulent transport affects ignition to detonation transition. Moreover, the shorter the turbulent eddy timescale, the longer the ignition transition to detonation and the weaker the detonation peak pressure. Therefore, the present results reveal that it is possible to use turbulent transport to control ignition to detonation transition in advanced engines.

Case	l(mm)	τ_t(ms)	εT	ξ_T	ξ_ϕ
1	1	83	2.09	0	5.4
2	1	333	2.09	0	5.4
3	1	83	3.14	4.5	0
4	1	83	2.09	6.8	0
5	0.5	83	3.14	4.5	0
6	2	83	3.14	4.5	0

Table 2 Test cases for different turbulence length scales (l), eddy timescale (τ), heat release rate (ε), and normalized temperature and equivalence ratio gradient (ξ)

5.3 Conclusion

Although low temperature ignition does not change the mixture compositions of the detonation boundary, it can significantly enhance and accelerate the knocking formation. As such, the low temperature ignition properties of a fuel will dominate the low speed pre-ignition in engines and the occurrence of super-knock. Turbulent transport affects ignition to detonation transition. The shorter the turbulent eddy timescale, the longer the ignition transition to detonation and the weaker the detonation peak pressure. Therefore, the present results reveal that it is possible to use turbulent transport to control ignition to detonation transition in advanced engines.

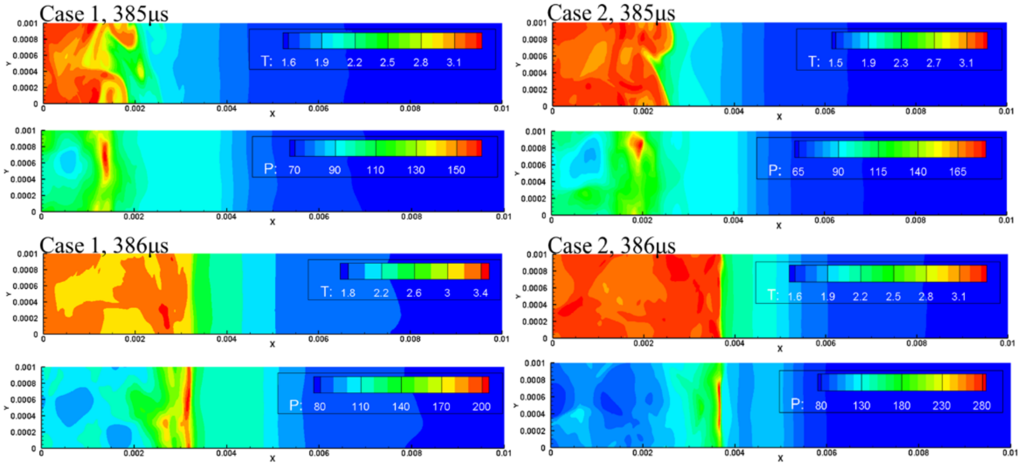

Fig.15 Comparison of temperature and pressure contours between Case 1 and Case 2.

6. Validated the efficacy of CO-DACT method in LES modeling in jet flames and development of Multiscale Adaptive Reduced Chemistry Solver (MARCS) for three-dimensional turbulent combustion modeling

6.1 Abstract

An on-the-fly mechanism reduction method named Correlated Dynamic Adaptive Chemistry (CO-DAC) was tested for large eddy simulations (LES) of Sandia Flame-D turbulent flames with detailed kinetic mechanisms. Predictions obtained with the LES/CO-DAC are in good agreement with the experimental data. Results showed that the usage of CO-DAC improved the computation efficiency. Moreover, it is demonstrated that the CO-DAC method provides reliable predictions of intermediate species and radicals. A Multiscale Adaptive Reduced Chemistry Solver (MARCS) is developed by integrating the Correlated Dynamic Adaptive Chemistry and Transport (CO-DACT) method with the Hybrid Multi-Timescale (HMTS) and G-Scheme methods, and the Full Speed Fluid Solver to conduct the efficient combustion modeling with detailed chemical kinetics. The preliminary results of ignitions and flame propagations demonstrate that the computational efficiency can be improved by orders of magnitude using CO-DACT method with HMTS and G-Scheme methods [4].

6.2 Results and Discussion

LES for Sandia Flame D (Methane/air turbulent diffusion flame) was simulated using the GRI-Mech 3.0 mechanism both with and without CO-DAC model reduction. Fig. 16 shows instantaneous contours of temperature and number of species and reaction in the locally reduced mechanism produced by CO-DAC reduction. Fig. 16 also shows that the size of the reduced mechanism is positively correlated to the local reactivity. The numbers of selected species and reactions are large in the flame region near the central line, demonstrating the active creation and destruction of intermediate species and radicals in this region. On the other hand, these numbers are small in the region away from the flame as there is mainly the post-burning production and the air co-flow. The average computational time per step without with CO-DAC is about a 33% reduction. Note that, the amount of reduced computational time in this study is not very large for CO-DAC. One major bottleneck is that we have to solve the large stiff reaction ODEs in this study.

Another bottleneck is the computation time required to compute the detailed transport properties. In the future, CO-DACT method should be used to accelerate the computation of transport properties.

Figure 17 shows the axial velocity and temperature profiles along the central line. There is small discrepancy between the results without and with CO-DAC reduction. The simulations are also in good agreement with the experiment data. The fluctuation of axial velocity is well reproduced. In addition, the temperature peak along the central line temperature is also well-predicted at about $x = 45d$ using detailed kinetic mechanism without reduction. The peak predicted using CO-DAC is shifted slightly downstream as compared to the no-reduction case.

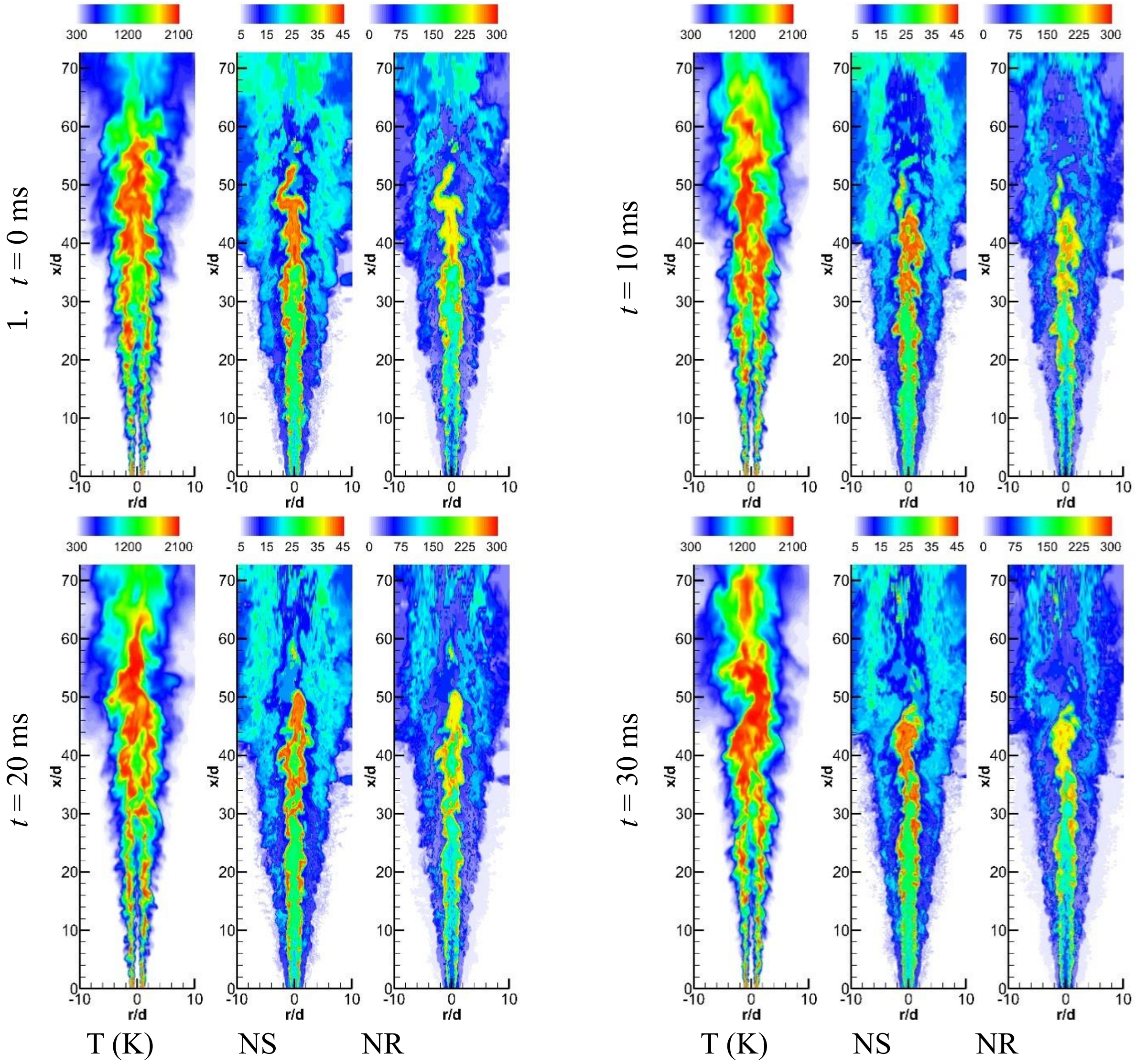

Fig. 16. Instantaneous contours at different computation times. In each diagram, temperature (T in K), the number of activated species (NS) and the number of reactions (NR) in reaction mechanism for flame-D are plotted from the left to the right.

6.3 Conclusion

The simulated results of the LES with CO-DAC reduction are in very good agreement with experimental data and that of the detailed mechanism. The results also accurately reproduced the distributions of the intermediate species and radicals. This good agreement demonstrates the accuracy of applying CO-DAC in LES modeling of turbulent flames. The number of species and reactions in local reduced mechanism is concentrated in the vicinity of the flame zone. CO-DAC reduction decreases the matrix dimensions in VODE solver and therefore reduces computational time. Future work needs to use an efficient chemistry integrator and adopt CO-DACT to further increase the computation efficiency.

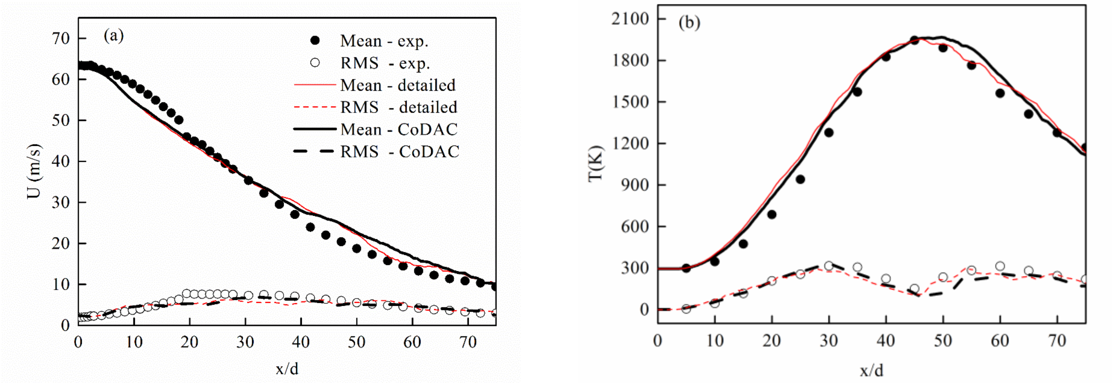

Fig. 16. Profiles of time-averaged (Mean) and root-mean-square (RMS) of (a) axial velocity and (b) temperature along the central line simulated using detailed kinetic mechanism without reduction (detailed) and with CO-DAC reduction (CO-DAC). The time-averaged and RMS experimental data (Exp.) are plotted as comparison.

7. Computational design of a new jet stirred reactor for low temperature chemistry study

7.1 Abstract

A new inwardly off-center shearing jet stirred reactor (IOS-JSR) for the study of low temperature chemistry is proposed and examined computationally for enhanced turbulent mixing and improved distribution of flow residence time in a jet stirred reactor for kinetic studies of real and alternative jet fuels. The IOS-JSR are compared with two traditional JSR designs, the outward cross-injector JSR and the concentric inward and outward JSR. The results show that the present IOS-JSR has significant improvement in terms of resulting mixture uniformity and residence time distribution. The distributions of residence time in traditional JSRs are much widened and long-tailed in longer residence time. Numerical results show that the mean residence time of the two classical JSRs has an uncertainty about 20%. The new IOS-JSR generates small vortices with different orientations and has a much narrower residence time distribution. The new IOS-JSR reduces the uncertainty in mean flow residence time to 8% and provides a better platform for kinetic studies of alternative and real jet fuels [5,6].

7.2 Results and summary

Fig.17 compares the geometry and simulated flow streamlines of three different JSRs, a) classical finger structured JSR, b) the newly proposed concentric inward and outward (CIAO) JSR, and c) the present inwardly off-center shearing (IOS) JSR, which has eight injection nozzles and four exhaust gas exit holes on the wall. The results showed that there is significant non-uniformity in the distributions of species and flow residence time in the traditional JSR designs. Compared to the two conventional JSRs, the present IOS-JSR has much improved performance in terms of mixture uniformity and narrower flow distribution time. There exist large recirculation zones in both CIAO JSR and Dagaut's JSR designs, where a large percentage of the mixture stay in there circulating vortex much longer than mean residence time. The ISO-JSR has the smallest standard deviation of residence time distributions among all three kinds of JSRs. As a result, the IOS-JSR will have great merits to improve the flow residence time distribution and contributes to the development and validation of chemical kinetics using a JSR.

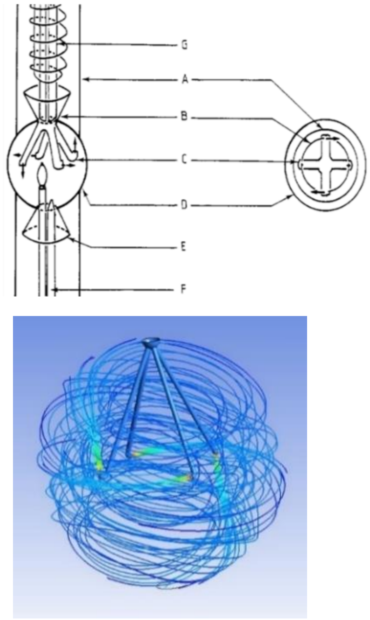

Fig. 17a. Geometry and stream lines of Dagaut's JSR

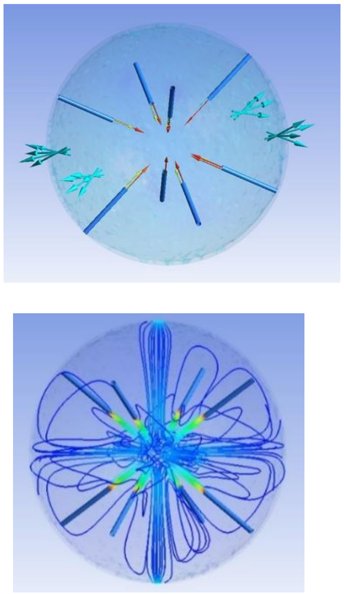

Fig. 17b. Geometry and streamlines of CIAO JSR

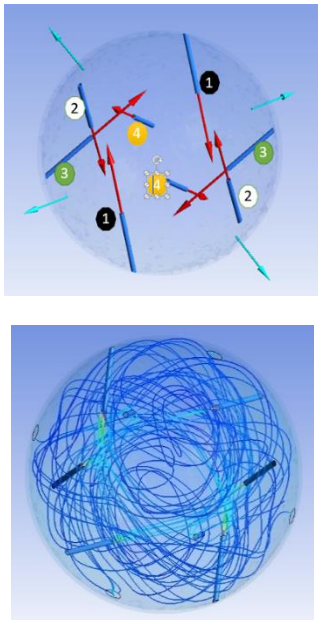

Fig. 17c. Geometry and streamlines of IOS JSR

The comparison of the flow residence time distributions of three different JSRs is shown in Fig. 18. The *x*-axis is the residence time on a Log scale and the y-axis is the percentage of corresponding particles. The particles are injected from the inlets and the initial positions are evenly distributed on the inlet surfaces. It can be seen from the Fig.18 that all of distribution functions in three JSRs have one main peak and a long tail in large residence time. Moreover, the position of the peak flow distribution time of each JSR is quite smaller than its average flow residence time. Note that for a perfect JSR, the location of the peak flow residence time should be exactly at the mean flow residence time under the fast and perfectly mixed assumption. The main reason for this discrepancy is due to the finite mixing time and dynamics of the vortexes inside the JSR. The theoretical result is calculated based on the assumption that all inlet flows will go through the whole volume with the same time histories. However, in a practical JSR, every flow particle will have different particle trajectories due to the effects of boundary layer and multiscale vortex motion. As such, some flow particles have shorter or faster pathways and others have longer or slower trajectories from inlets to outlets**.**

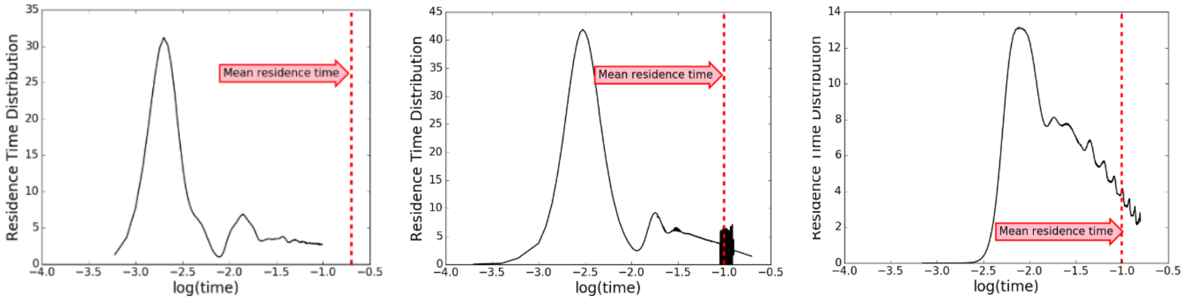

Fig. 18 a. Residence time distribution for Dagaut's JSR, b: residence time distribution for CIAO JSR, c: residence time distribution for IOS JSR.

7.3 Conclusion

A new concept of the inwardly off-center shearing (IOS) Jet Stirred Reactor is proposed and examined numerically in comparing with two traditional JSR designs, the CIAO JSR and OCI JSR for achieve improved turbulent mixing and narrowly defined distribution of flow residence time as well as well-defined mean flow residence time. The results showed that there is significant non-uniformity in the distributions of species and flow residence time in the traditional JSR designs. Compared to the two conventional JSRs, the present IOS-JSR has much improved performance in terms of mixture uniformity and narrower flow distribution time. There exist large recirculation zones in both CIAO JSR and Dagaut's JSR designs, where a large percentage of the mixture stay in there circulating vortex much longer than mean residence time, while the rest of mixture exits reactor directly through shortened streamlines from inlets to outlets. In contrast, the present IOS-JSR creates a fully mixed environment using inwardly shearing jets which cover the whole volume of reactors and avoid generating large vortexes at the same time. Consequently, the ISO-JSR has the smallest standard deviation of residence time distributions among all three kinds of JSRs. As a result, the IOS-JSR will have great merits to improve the flow residence time distribution and contributes to the development and validation of chemical kinetics using a JSR. In addition, its simplified geometry enables optical diagnostics with both in-situ ultra-violet and infra-red lasers which can significantly extend the measure capability of the current JSRs for kinetic studies of jet fuels.

8. References

1. Weiqi Sun and Yiguang Ju, (2017); A multi-timescale and correlated dynamic adaptive chemistry and transport (CO-DACT) method for computationally efficient modeling of jet fuel combustion with detailed chemistry and transport, Combustion and Flame 184 (2017) 297–311.

2. Tianhan Zhang, Weiqi Sun, Yiguang Ju, (2017); Multi-scale Modeling of Detonation Formation with Concentration and Temperature Gradients in n-Heptane/Air Mixtures, Proceedings of the Combustion Institute, 36(1), pp.1539-1547.

3. Tianhan Zhang, Weiqi Sun, Liang Wang, Yiguang Ju, "Effects of Low-Temperature Chemistry and Turbulent Transport on Knocking Formation for Stratified Dimethyl Ether/Air Mixtures, Combustion and Flame, Vol.200, 2019:342-353.

4. Liu, Z., Han, W., Kong, W. and Ju, Y., 2018. LES modelling of turbulent non-premixed jet flames with correlated dynamic adaptive chemistry. *Combustion Theory and Modelling*, 22, pp.1-20. https://doi.org/10.1080/13647830.2018.1447148
5. Yiguang Ju, Christopher B. Reuter, Omar R. Yehia, Tanvir I. Farouk, and Sang Hee Won, Dynamics of Cool Flames, Progress of Energy and Combustion Science, 75 (2019), 100787. https://doi.org/10.1016/j.pecs.2019.100787.
6. Zhang, T., Zhao, H. and Ju, Y., 2018. Numerical Studies of Novel Inwardly Off-Center Shearing Jet-Stirred Reactor. *AIAA Journal*, 56, pp.1-5. https://doi.org/10.2514/1.J057293